

A Non-axisymmetric Magnetorotational Instability of a Purely Toroidal Magnetic Field

Rainer Hollerbach¹ and Günther Rüdiger, Manfred Schultz, D. Elstner²

¹*Department of Applied Mathematics,
University of Leeds, Leeds, LS2 9JT, United Kingdom*

²*Astrophysikalisches Institut Potsdam,
An der Sternwarte 16, D-14482 Potsdam, Germany*

(Dated: August 16, 2018)

Abstract

We consider the flow of an electrically conducting fluid between differentially rotating cylinders, in the presence of an externally imposed toroidal field $B_0(r_i/r) \hat{e}_\phi$. It is known that the classical, axisymmetric magnetorotational instability does not exist for such a purely toroidal imposed field. We show here that a non-axisymmetric magnetorotational instability does exist, having properties very similar to the axisymmetric magnetorotational instability in the presence of an axial field.

PACS numbers: 47.20.-k, 47.65.+a, 95.30.Qd

The magnetorotational instability (MRI) is a mechanism whereby a hydrodynamically stable differential rotation flow may be destabilized by the addition of a magnetic field. An obvious question then is whether different orientations of the field yield different types of instability, or the same, or none at all. The original view was that the axial component of the field is the only important one, with any azimuthal component playing no essential role, and incapable of producing any instabilities on its own [1, 2]. This view was altered by the discovery that a mixed axial and azimuthal field yields instabilities quite different in many ways from those found with a purely axial field [3, 4]. In this letter we show that even a purely azimuthal field yields an MRI, and compare its properties with the previously known types.

While its most important application is to astrophysical accretion disks [2], the MRI was originally discovered in the much simpler Taylor-Couette problem, consisting of the flow between differentially rotating cylinders [1]. Because of its relative simplicity, this geometry has proven particularly amenable both to theoretical analyses of the MRI [5, 6, 7], as well as to its recent experimental realization [8, 9]. We too shall examine the MRI in this context.

Consider therefore an electrically conducting fluid confined between two concentric cylinders of radii r_i and r_o , rotating at rates Ω_i and Ω_o , chosen to satisfy $\Omega_o r_o^2 > \Omega_i r_i^2$. That is, the angular momentum increases outward, so by the familiar Rayleigh criterion the flow is hydrodynamically stable, with the angular velocity given by

$$\Omega(r) = A + B/r^2, \tag{1}$$

where

$$A = \frac{\Omega_o r_o^2 - \Omega_i r_i^2}{r_o^2 - r_i^2}, \quad B = \frac{r_i^2 r_o^2 (\Omega_i - \Omega_o)}{r_o^2 - r_i^2}. \tag{2}$$

In this work we will fix $r_o = 2r_i$ and $\Omega_o = \Omega_i/2$, so A and B simplify to $\frac{1}{3}\Omega_i$ and $\frac{2}{3}\Omega_i r_i^2$, respectively. The essence of the MRI then is to ask whether the addition of a magnetic field can destabilize this flow.

If the imposed field is purely axial, $\mathbf{B}_0 = B_0 \hat{\mathbf{e}}_z$, the profile (1) can be destabilized, provided the rotation rates are sufficiently great, and the field strength B_0 is neither too weak nor too strong [5, 6]. Specifically, the magnetic Reynolds number $\text{Rm} = \Omega_i r_i^2 / \eta$, where η is the magnetic diffusivity, must exceed $O(10)$, and the Lundquist number $S = B_0 r_i / \eta \sqrt{\rho \mu}$, where ρ is the density and μ the permeability, must be around 3 – 10.

In contrast, if the imposed field is mixed axial and azimuthal, $\mathbf{B}_0 = B_0 \hat{\mathbf{e}}_z + \beta B_0 (r_i/r) \hat{\mathbf{e}}_\phi$, where β is around 1–10, then the profile (1) can again be destabilized, but at very different rotation rates and field strengths [3, 4]. The relevant parameter measuring the rotation rates is now not the magnetic Reynolds number, but rather the hydrodynamic Reynolds number $\text{Re} = \Omega_i r_i^2 / \nu$, where ν is the viscosity. Similarly, the parameter measuring the field strength is not the Lundquist number, but instead the Hartmann number $\text{Ha} = B_0 r_i / \sqrt{\rho \mu \eta \nu}$. The MRI sets in when $\text{Re} \gtrsim O(10^3)$, and $\text{Ha} \approx O(10)$.

To compare these results, we note that the two sets of parameters are related by $\text{Re} = \text{Rm} \text{Pm}^{-1}$ and $\text{Ha} = \text{S} \text{Pm}^{-1/2}$, where $\text{Pm} = \nu / \eta$ is the magnetic Prandtl number, a material property of the fluid. Typical values for liquid metals are $O(10^{-6})$. Translating the results for the purely axial field, we thus obtain $\text{Re} \gtrsim O(10^7)$ and $\text{Ha} \approx O(10^4)$, both several orders of magnitude greater than for the mixed field. It is perhaps not surprising then that the MRI has been obtained experimentally for the mixed field [8, 9], but not (yet) for the purely axial field [5].

As different as they are, one feature these two types of MRI have in common is that they are both axisymmetric. Non-axisymmetric modes have also been explored, for both the purely axial [7] as well as the mixed fields [4]. For a purely axial field the relevant parameters are still Rm and S , but the critical values Rm_c are somewhat larger than for the axisymmetric modes, indicating that the axisymmetric MRI is the most unstable mode. For mixed fields, one finds — perhaps somewhat surprisingly — that adding an azimuthal component now has minimal effect, certainly far less than the reduction by four orders of magnitude found for the axisymmetric modes. Evidently the relevant parameters continue to be Rm and S , rather than Re and Ha .

What we wish to show in this letter then is that for these non-axisymmetric modes, one can impose a purely azimuthal field, $B_0 (r_i/r) \hat{\mathbf{e}}_\phi$, and still obtain an MRI, having all the characteristics of the previous non-axisymmetric types of MRI [4, 7]. To this end, we solve the linear stability equations

$$\text{Rm} \frac{\partial \mathbf{b}}{\partial t} = \nabla^2 \mathbf{b} + \nabla \times (\mathbf{u} \times \mathbf{B}_0) + \text{Rm} \nabla \times (\mathbf{U}_0 \times \mathbf{b}), \quad (3)$$

$$\text{Re} \frac{\partial \mathbf{u}}{\partial t} = -\nabla p + \nabla^2 \mathbf{u} + \text{Ha}^2 (\nabla \times \mathbf{b}) \times \mathbf{B}_0 + \text{Re} (\mathbf{U}_0 \times \nabla \times \mathbf{u} + \mathbf{u} \times \nabla \times \mathbf{U}_0), \quad (4)$$

where $\mathbf{U}_0 = r\Omega(r) \hat{\mathbf{e}}_\phi$ is the profile (1) whose stability we are exploring, and $\mathbf{B}_0 = B_0 (r_i/r) \hat{\mathbf{e}}_\phi$ is the imposed azimuthal field. Length has been scaled by r_i , time by Ω_i^{-1} , \mathbf{U}_0 and \mathbf{u} as

$r_i\Omega_i$, \mathbf{B}_0 as B_0 , and \mathbf{b} as $\text{Rm}B_0$.

Taking the t , z and ϕ dependence to be of the form $\exp(\sigma t + ikz + im\phi)$, and using also $\nabla \cdot \mathbf{b} = 0$ to eliminate b_z , the r and ϕ components of (3) become

$$\text{Rm} \sigma b_r = \nabla^2 b_r - r^{-2} b_r - 2imr^{-2} b_\phi + imr^{-2} u_r - \text{Rm} im\Omega b_r, \quad (5)$$

$$\text{Rm} \sigma b_\phi = \nabla^2 b_\phi - r^{-2} b_\phi + 2imr^{-2} b_r + imr^{-2} u_\phi + 2r^{-2} u_r - \text{Rm} im\Omega b_\phi + \text{Rm} \Omega' r b_r, \quad (6)$$

where primes denote d/dr . The components of (4) have a similar structure, but we will not need to refer to them in the subsequent discussion, and hence do not list them. The boundary conditions associated with (3) and (4) are

$$b_r = b'_\phi + r^{-1} b_\phi = u_r = u_\phi = u_z = 0 \quad (7)$$

at $r = r_i$ and r_o , corresponding to perfectly conducting, no-slip walls. The resulting one-dimensional linear eigenvalue problem is solved by finite differencing in r , as in [7].

Figure 1 shows stability curves for $m = 1$, the only mode that appears to become unstable. We see how an MRI exists that is remarkably similar to some of the results described above. In particular, as $\text{Pm} \rightarrow 0$, the relevant parameters are clearly once again Rm and S , with the MRI arising if $\text{Rm} \gtrsim 80$, and $S \approx 40$ yielding the lowest value of Rm_c . The specific numbers are roughly an order of magnitude greater than for the axisymmetric MRI in the axial field, but the basic scalings, and even the detailed shape of the instability curves, are identical.

Figure 2 shows the real and imaginary parts of σ in the unstable regime. Remembering that time has been scaled by Ω_i^{-1} , we see that we obtain growth rates as large as $0.05\Omega_i$. So again, while the particular number 0.05 is about an order of magnitude smaller than for the axisymmetric MRI in the axial field, this non-axisymmetric MRI is clearly also growing on the basic rotational timescale.

To understand why this non-axisymmetric MRI exists even for a purely toroidal field \mathbf{B}_0 , for which it is known that the axisymmetric MRI fails [1, 2], we need to consider the details of (5) and (6). In particular, note that for $m = 0$, b_r completely decouples from everything else, and inevitably decays away. Without b_r though, the MRI cannot proceed, as it relies on the term $\text{Rm} \Omega' r b_r$ in (6). In contrast, for $m = 1$, b_r is coupled both to b_ϕ , coming from $\nabla^2 \mathbf{b}$, and to u_r , from $\nabla \times (\mathbf{u} \times \mathbf{B}_0)$. And once b_r is coupled to the rest of the problem,

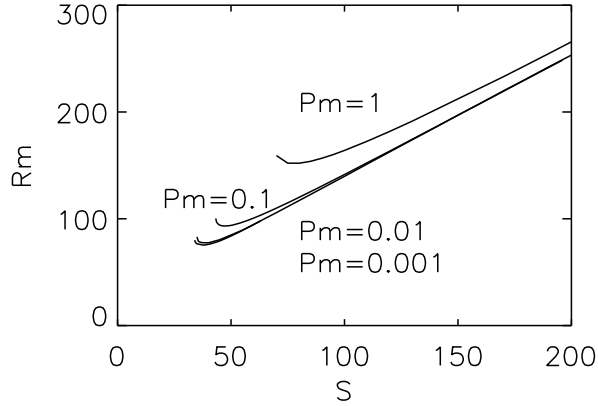


FIG. 1: The critical magnetic Reynolds number for the onset of the MRI, as a function of the Lundquist number, for the different values of Pm indicated. $m = 1$, $r_o/r_i = 2$, $\Omega_o/\Omega_i = 0.5$.

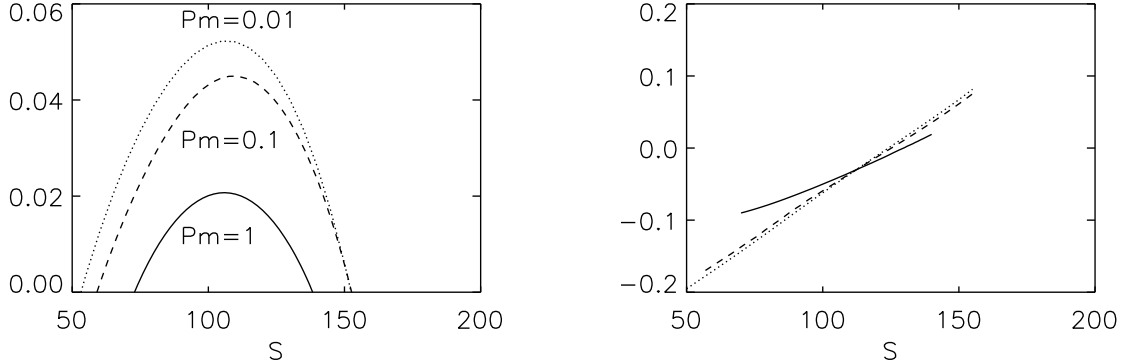


FIG. 2: The real (top) and imaginary (bottom) parts of σ , as functions of S, with Rm fixed at 200. The real part corresponds to the growth rate, the imaginary part to the azimuthal drift rate.

the term $\text{Rm} \Omega' r b_r$ then allows the MRI to develop. Figure 3 presents an example of these solutions, indicating how all three components of both \mathbf{u} and \mathbf{b} are indeed present.

There is however one aspect that is not entirely clear from this analysis, namely why this non-axisymmetric MRI actually requires the term $\text{Rm} \Omega' r b_r$ at all. In particular, the axisymmetric MRI with a mixed field does *not* rely on it, but instead on the term $2r^{-2}u_r$, coming from $\nabla \times (\mathbf{u} \times \mathbf{B}_0)$ rather than $\text{Rm} \nabla \times (\mathbf{U}_0 \times \mathbf{b})$ [3]. The non-axisymmetric MRI is evidently more like the axisymmetric MRI with a purely axial field, which also requires the term $\text{Rm} \Omega' r b_r$, because in that case the term $2r^{-2}u_r$ is absent.

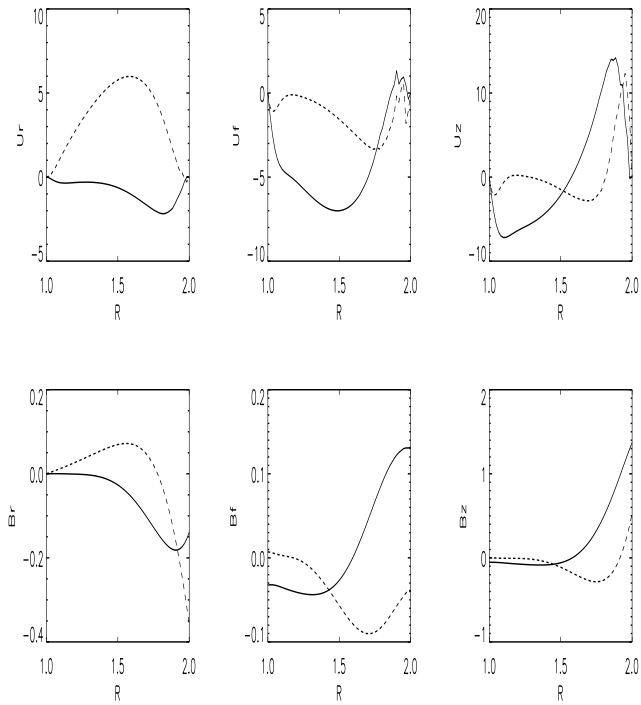


FIG. 3: The marginally stable solution at $\text{Pm} = 0.1$, $S = 47.4$ and $\text{Rm} = 93$ (see Fig. 1). From left to right the r , ϕ and z components of \mathbf{u} (top) and \mathbf{b} (bottom). The real parts are solid, imaginary parts dashed. Note how both \mathbf{u} and \mathbf{b} have the z components largest. The azimuthal wavenumber is $k = 1.88$.

To summarize then, we have shown that even if the externally imposed magnetic field is purely toroidal, one still obtains an MRI, simply non-axisymmetric rather than axisymmetric. In other respects though this new instability is remarkably like the classical axisymmetric MRI with a purely axial field, indeed far more like it than the axisymmetric MRI with a mixed field, which yielded fundamentally different scalings. In contrast, the parameters here continue to be Rm and S , just as in the classical MRI.

Note though that attempting to obtain this non-axisymmetric MRI in a laboratory experiment would be even more difficult than attempting to obtain the classical axisymmetric MRI in an axial field. First, the required rotation rates would be even greater, $\text{Re} \gtrsim O(10^8)$, with all the difficulties that entails [10]. Even more daunting, imposing an azimuthal field of the required strength, $\text{Ha} \approx O(10^5)$, would require a current along the central axis in excess of 10^6 A, surely far beyond any feasible experiment.

This new non-axisymmetric MRI could have astrophysical applications though, since many astrophysical objects do have predominantly azimuthal fields, in which case the results presented here suggest that this non-axisymmetric MRI could be preferred over the axisymmetric MRI.

Despite the similarities in their fundamental scalings, the fact that the classical MRI is axisymmetric, whereas this new MRI is non-axisymmetric, means the nonlinear equilibration, and hence the associated angular momentum transport, are potentially quite different, which could again have astrophysical implications. Work on this is currently in progress.

Finally, one might ask how the results presented here change if one allows for a more general toroidal field profile, $\mathbf{B}_0 = (c_1 r^{-1} + c_2 r) \hat{\mathbf{e}}_\phi$, where the term $c_2 r$ corresponds to an electric current flowing through the fluid itself, and not just along the central axis. Eq. (4) then contains an additional term $\text{Ha}^2(\nabla \times \mathbf{B}_0) \times \mathbf{b}$, which opens up the possibility of instabilities driven entirely by this current $\nabla \times \mathbf{B}_0$, without any rotation necessarily present at all [11]. Understanding how these current driven instabilities (also $m = 1$) interact with the magnetically catalyzed but ultimately rotationally driven MRI presented here is also in progress.

This work was supported by the German Leibniz Gemeinschaft, under program SAW.

-
- [1] E. P. Velikhov, *Sov. Phys. JETP* **36**, 995 (1959).
 - [2] S. A. Balbus and J. F. Hawley, *Astrophys. J.* **376**, 214 (1991).
 - [3] R. Hollerbach and G. Rüdiger, *Phys. Rev. Lett.* **95**, art no 124501 (2005).
 - [4] G. Rüdiger, R. Hollerbach, M. Schultz and D. Shalybkov, *Astron. Nachr.* **326**, 409 (2005).
 - [5] H. T. Ji, J. Goodman, and A. Kageyama, *Mon. Not. Roy. Astron. Soc.* **325**, L1 (2001).
 - [6] G. Rüdiger and Y. Zhang, *Astron. Astrophys.* **378**, 302 (2001).
 - [7] G. Rüdiger, M. Schultz, and D. Shalybkov, *Phys. Rev. E* **67**, art no 046312 (2003).
 - [8] F. Stefani, T. Gundrum, G. Gerbeth, G. Rüdiger, M. Schultz, J. Szklarski and R. Hollerbach, *Phys. Rev. Lett.* **97**, art no 184502 (2006).
 - [9] G. Rüdiger, R. Hollerbach, F. Stefani, T. Gundrum, G. Gerbeth and R. Rosner, *Astrophys. J.* **649**, L145 (2006).
 - [10] R. Hollerbach and A. Fournier, in *AIP Conf. Proc.* 733, MHD Couette Flows: Experiments

and Models, ed. R. Rosner, G. Rüdiger and A. Bonanno, (New York: AIP), 114 (2004).

[11] R. J. Tayler, Mon. Not. Roy. Astron. Soc. **161**, 365 (1973).